# Effect of mechanical and thermochemical tool steel substrate pre-treatment on diamond-like carbon (DLC) coating durability

Daniel Toboła [a], Tomasz Liskiewicz [b], Liuquan Yang [c], Thawhid Khan [b], Łukasz Boroń [a]

[a] *Łukasiewicz Research Network - Krakow Institute of Technology, Zakopianska 73 Str., 30-418 Krakow, Poland*
[b] *Department of Engineering, Manchester Metropolitan University, Manchester M15 6BH, United Kingdom*
[c] *School of Mechanical Engineering, University of Leeds, Leeds, LS2 9JT, United Kingdom*

## ARTICLE INFO

## ABSTRACT

Diamond-like carbon (DLC) coatings are becoming well established across many industrial sectors including aerospace, automotive, oil and gas, and cold-forming tools. While DLC coatings exhibit good mechanical properties and a low coefficient of friction, the coating–substrate systems may suffer from insufficient wear resistance. This paper describes the effect of mechanical and thermochemical tool steel substrate pre-treatment on DLC coating durability. We have investigated two tool steel substrates, Sverker 21 (AISI D2) and an advanced powder metallurgy alloyed steel Vanadis 8. Initially, the substrates were heat treated in a vacuum furnace and gas quenched resulting in hardness of $59 \pm 1$ and $64 \pm 1$ Hardness Rockwell C (HRC) respectively. Subsequently, the samples were subjected to mechanical turning and burnishing with 130 N and 160 N forces, using diamond composite tools with a ceramic bonding phase. Afterwards, a plasma-assisted vacuum nitriding process in a physical vapour deposition (PVD) coating chamber, as a pre-treatment for subsequent DLC coating deposition, was carried out. Coated samples were subjected to a series of ball-on-disc wear tests against $Al_2O_3$ and $Si_3N_4$ counterparts. X-ray diffraction, instrumented indentation and scanning electron microscopy were employed to examine the mechanical and chemical properties of the wear scars. Selected variable factors, including the type of steel, the burnishing force and the type of counterbody material, were analysed in order to correlate them with the durability of DLC coating deposited on a pre-treated steel substrate. The effect of sequential processes used as pre-treatment on DLC coating durability was demonstrated. The wear resistance was over 180 (Sverker 21 substrate) and 10 (Vanadis 8 substrate) times greater against the $Al_2O_3$ counterbody for samples subjected to the following treatment: turning + burnishing with 160 N force + vacuum nitriding + DLC coating, comparing with the sample after grinding. The results are discussed in light of improving the cold-forming tools' tribological performance.

## 1. Introduction

The global metal cutting tools market was valued at $22.2bn in 2018 and is projected to grow at a compound annual growth rate (CAGR) of 8.8% to reach $38.3bn by 2024 [1]. Machining is a subtractive manufacturing process using cutting tools to manufacture products through material removal to specified shapes and properties. With any manufacturing process, there is a need for tool longevity and finish quality (smooth surface, dimensional stability). Machining operations are being constantly optimized with new difficult-to-machine workpiece materials, strict environmental requirements, increased productivity demands and manufacturing costs. Increases in cutting speed lead to an

increase in tool–workpiece interaction, along with increases in the temperature and wearing of the tool. To reduce wear and prevent fracture, the tool must be ductile and hard, which presents contradictory demands – a material is either hard and with poor ductility, or vice versa. A solution to this problem is to protect the ductile tool with hard coating. The substrate provides resistance to fracture, while hard coating protects the cutting edge against abrasive and mild adhesive wear. The coating can also help to reduce tool temperature by reducing the friction between chip and rake face of a tool [2,3].

Cutting tools account for 3% of the overall machining costs and the production cost per component can be reduced by 1% with a 50% increase in tool durability. Efficient tools can reduce downtime costs due

to tool changes, with effective machining further improved by innovative tools solutions. The development of new coatings and coating systems is the first step towards an increased productivity in machining [4]. Tool coating development has been focused on wear protection against abrasion and adhesion. With machining of hard-to-cut alloys and higher cutting temperatures generated, research and development has shifted towards the high temperature properties of coatings and tool substrates, and the need to withstand mechanical and thermal loads. Beside tool coatings providing oxidation protection, they must also function as a diffusion barrier between the tool and the workpiece. The requirements for the tool substrate are demanding because of the cyclic loading conditions, which can lead to thermally and/or mechanically induced crack formation [4].

The effectiveness of tools (tool performance, accuracy of the product and durability) for cold forming depends on the type of tool work, conditions associated with formed material and technical condition of the equipment used in production (the press). The choice of tool material and technology used in tool production are typically verified through industrial testing and behaviour observation through its lifetime. In commercial practice, wear processes are very complex, with different forms of surface damage dominating the various stages of tool life [5]. The following factors are attributed as important for the course of wear of tools for cold working: a) the chemical composition of the steel and the method of its manufacturing; b) heat treatment, the material structure, especially the resulting carbide phase; c) the operating conditions of the tool; d) the process of surface preparation (surface engineering).

The most commonly used mechanical finishing operations of tool steels are turning, milling, grinding, polishing, smoothing and various types of burnishing (rolling and sliding burnishing, shot peening) [6–11]. In traditional manufacturing processes, the finishing operation of tools and machine parts, of which hardness after heat treatment is higher than 45 HRC and even 60 HRC, is often grinding. For several decades in many industries, e.g., automotive, bearing and die manufacturing, processes of grinding are gradually replaced by so-called 'hard machining' (HM) [12]. However, HM does not always meet the requirements for the expected surface quality. The way of overcoming these technological barriers is often burnishing, which is applied both to the turned and milled surfaces [12]. Among the different methods of finishing, the main distinguishing feature of burnishing is the use of surface plastic deformation.

Hard coatings have become an integral part of modern tool technology, with the aim of extending tool life and increasing productivity. From a functional point of view, the most important coating properties are hot hardness, surface adhesion and chemical stability. It has been demonstrated that the application of physical vapour deposition (PVD) coating systems can effectively decrease the friction between the cutting tool and workpiece [13]. It should also be noted that among the industrial surface engineering methods, thermo-chemical treatments, including nitriding, play a dominant role [14–16].

One typical coating applied through PVD method is diamond-like carbon (DLC) coating. DLC coatings are widely used in applications where low friction and high wear resistance are of prime importance [17].

The composition of diamond-type bonded carbon ($sp^3$), graphite-type bonded ($sp^2$) and other elements like hydrogen, metals or non-metals, determine the hardness and durability of the coating. In manufacturing, DLC films have proved to be excellent cutting tool coatings for machining non-ferrous metals, non-metal materials and composite materials, as they demonstrate excellent tribological, electrical and chemical properties. DLC can be deposited on majority types of tool materials enabling dry machining and semi-dry machining, which has a positive environmental impact [18].

The key disadvantage of DLC coating on cutting tools is its poor adhesion to the substrate. Studies have recommended an intermediate layer between the cutting tool substrate and DLC coating to improve

adherence [18]. The main aim of the multilayer system is to create a complementary combination of properties for a wide range of machining conditions providing adequate protection against mechanical wear, high temperatures and chemical interactions [3].

To further improve the cohesion of coating/substrate interface, the tool substrate can be pre-treated, using processes such as blasting and acid etching [19]. Other pre-treatments could include plasma nitriding to increase the hardness of the cutting tool substrate. However, high hardness differences between the coating and substrate can lead to a loss of adhesion as the substrate deforms during machining. Hence, plasma nitriding would produce a hardness gradient between the coating and substrate, improving the adhesion [20].

In the present paper, we have studied the effect of mechanical and thermochemical steel substrate pre-treatments on DLC coating durability and their correlations with the tribological properties of Sverker 21 (AISI D2) and Vanadis 8 tool steels.

## 2. Experimental methods

### 2.1. Substrate materials

The chemical composition of steels used in this project are given in Table 1. Sverker 21 is a conventional steel, while Vanadis 8 is classified as advanced powder metallurgy (P/M) alloyed steel. Vanadis 8 is distinguished by high content of C and V, unattainable in steels processed by conventional metallurgic technology. Samples (ø32 × 12 mm) were machined and then subjected to heat treatment in vacuum furnaces with gas quenching (Table 2).

### 2.2. Mechanical surface treatments

After undergoing the heat treatment, specimens were subjected to selected mechanical surface modification processes, namely grinding (G), hard turning (T) and hard turning followed by burnishing (T + B). In the second stage, vacuum nitriding (VN) and DLC coating deposition were carried out (see Fig. 1 and Section 2.3). This multi-stage surface modification process was applied on both substrate steels. Front face grinding with cubic boron nitride (CBN) wheels with resinous bond was carried out on a universal tool grinder type 3E642. A Mori Seiki NL2000SY turning-milling CNC centre, equipped with a fixing system described in earlier work [21], was used for hard turning and slide burnishing on samples' end faces. Hard turning was carried out using polycrystalline cubic boron nitride (PCBN) cutting inserts, while slide diamond burnishing was carried out using diamond tools. High pressure-high temperature (HP-HT) Bridgman type apparatus was used to obtain diamond composites with ceramic bonding phase, namely titanium diboride ($TiB_2$). Compacts were sintered at the pressure of 7.8 ± 0.2 GPa at 1800 ± 50 °C for 20 s. Subsequently, their spherical shapes were formed by electrical discharge machining (EDM).

Bearing in mind the difficulties in machine finishing of hardened tool steels and the fact that machining as a finishing operation cannot always provide an appropriate state of surface layer, the use of slide burnishing (see Fig. 2) is justified. The benefits of using slide burnishing were described in detail by Maximov et al. [22,23].

### 2.3. Thermochemical surface treatment with DLC coating deposition

The specimens were cleaned in the ultrasonic bath with ethanol for 15 min and fixed in the coating substrate table in the vacuum chamber

**Table 1**
Chemical composition (wt%) of Sverker 21 and Vanadis 8 tool steels.

| Steel | C | Si | Mn | Cr | Mo | V |
|---|---|---|---|---|---|---|
| Sverker 21 | 1.55 | 0.3 | 0.4 | 11.8 | 0.8 | 0.8 |
| Vanadis 8 | 2.3 | 0.4 | 0.4 | 4.8 | 3.6 | 8.0 |

**Table 2**
Heat treatment parameters for examined tool steels.

|  | Sverker 21 | Vanadis 8 |
|---|---|---|
| Austenitizing | 1030 °C | 1180 °C |
| First tempering | 500 °C, 2 h | 560 °C, 2 h |
| Second tempering | 500 °C, 2 h | 560 °C, 2 h |
| Resulting hardness | 59 ± 1 HRC | 64 ± 1 HRC |

with two-fold rotation. The process was carried out in a Hauzer Flexi-Coat 850 deposition system. It involved two steps in the vacuum chamber without taking the specimens out during the process. Step one was the plasma-assisted vacuum nitriding. The chamber was pumped down to a based pressure of $5 \times 10^{-5}$ mbar and then heated up to 480 °C for two hours. The specimens were further cleaned in the vacuum by plasma surface etching for 45 min using a 200 V bias, 60 A anode current and 50 sccm argon gas plasma. The plasma nitriding was then conducted for 150 min with a very tight temperature window between 490 °C – 500 °C. Plasma-assisted vacuum nitriding employed a bias voltage of 120 V, bias plasma voltage of 50 V, gas flow rates of 70 sccm of nitrogen and 70 sccm of argon. The chamber was subsequently cooled down to 200 °C in the vacuum after the nitriding step. Step two was the coating step, with a structure of Cr/WC/W-C:H/DLC. It started from a Cr layer deposition with an Ar flowrate of 130 sccm using a magnetron sputtering process. The power used was 3 kW for the Cr layer and the deposition time was 30 min. Another 30 min of transition layer involved

ramping down Cr magnetron power from 3 kW to 0.5 kW and ramping up WC magnetron power from 0.5 kW to 3 kW. The gas flowrate was 110 sccm during this Cr/WC ramping stage. The W-C:H layer deposition was 45 min, which involved switching off the Cr magnetron completely and ramping up the acetylene gas from 8 sccm to 30 sccm for 30 min. Finally, the pure DLC coating was deposited with acetylene gas only by plasma-enhanced chemical vapour deposition (PECVD) for four hours. The bias voltage used was 740 V and the acetylene gas flowrate was 270 sccm. The chamber was subsequently cooled down to room temperature and unloaded.

Both the plasma nitriding and the DLC coating deposition processes were previously developed at the University of Leeds. Surface treatment optimization was not the scope of this paper, hence standard coating recipes were chosen in this study [24].

### 2.4. Mechanical and surface characterization

Metallographic structures after selected treatments were characterized by a scanning electron microscope (SCIOS FEI), equipped with an energy-dispersive spectrometer (EDS) using polished specimen cross-sections. Moreover, observations of the DLC coating and formed nitride layer were conducted in a bright field using an AxioObserver Zm1 tabletop metallographic microscope (Carl Zeiss). The images were recorded with the AxioVisio software. Wear tracks were observed and analysed with a different type of scanning electron microscope (JEOL
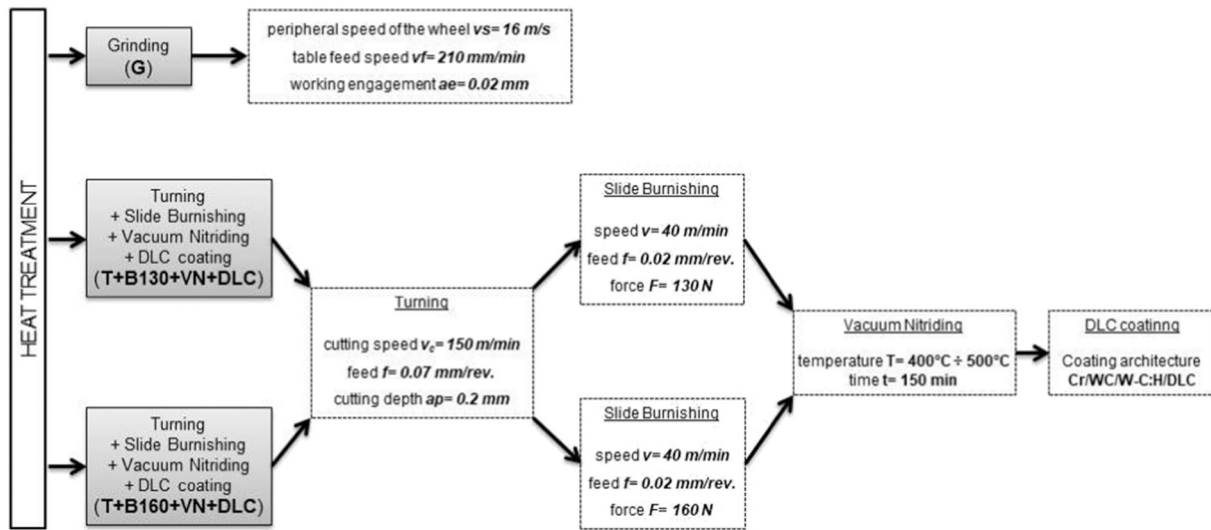


**Fig. 1.** Types of surface treatment processes with parameters applied on both types of steel.
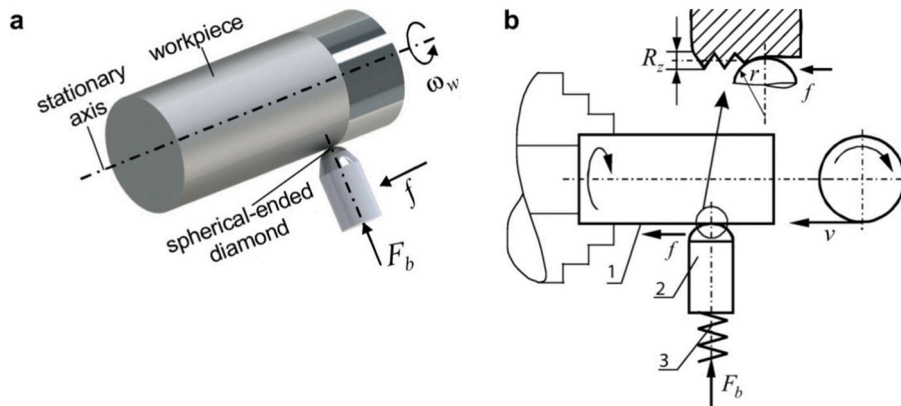


**Fig. 2.** Scheme (a) and kinematics (b) of slide burnishing process, based on [22]

type JSM-6460LV) equipped with an INCA EDS (energy dispersive X-ray spectrometer).

The Raman spectroscopy (NTEGRA SPECTRA, NT-MDT Europe) was used for characterization of DLC coating. The Raman spectra were taken under ambient conditions using a diode-pumped solid-state laser with a wavelength of 473 nm. The incident laser power was 50 mW, with the spot size ~1 μm in diameter and the exposure time of 300 s.

Microhardness distribution of the nitrided layers was determined using a FM 7 tester (Future Tech. Corp., Japan) using Vickers indented and 100 g load.

Hardness (H) and Young modulus (E) of DLC coating were measured using the Anton Paar STEP 500 platform with Berkovich diamond indenter by applying the Oliver-Pharr analysis [25]. The following parameters were used: max load = 10 mN, loading/unloading rate = 20 mN/min, with a 5 s pause. Eight repeats were carried out on each sample.

Finally, scratch tests were performed using Anton Paar's multifunctional measurement platform OPX for micromechanical properties. Scratch tests were carried out with a Rockwell indenter, $R = 0.1$ mm, with an incremental load from 0.03 N to 5 N over a 2 mm long track.

### 2.5. Tribological testing

The wear resistance was evaluated by employing the ball-on-disc method, using a CETR UMT-2MT universal mechanical tester. The loading mechanism applied a controlled load $F_n$ to the ball holder and the friction force was measured continuously during the test using an extensometer. Brostow and Hagg Lobland [26] described in detail how to use this technique. For each test, a new ball was used. The ball and discs were washed in ethyl alcohol and dried. The size of the disc-shaped samples with the surface flatness and parallelism within 0.02 mm is shown in Fig. 3a. Parameters applied during wear tests are given in Table 3. Calculated maximum Hertzian contact pressures for applied counterbodies were:

a) ~1565 MPa ➔ $Al_2O_3$ and ~1525 MPa ➔ $Si_3N_4$ for Sverker 21 conventional steel,
b) ~1620 MPa ➔ $Al_2O_3$ and ~1590 MPa ➔ $Si_3N_4$ for Vanadis 8 P/M steel.

We assumed that the contact pressure did not exceed the yield strength of investigated steels, which eliminated the plastic deformation.

Using a contact profilometer TOPO 01 equipped with a measuring head with a diamond tip radius of 2 μm and a cone angle of 60°, surface roughness parameters of samples and the loss of material after tribological tests were determined according to the ISO20808:2004E standard (as described in detail in our previous work [27]). Measurements of
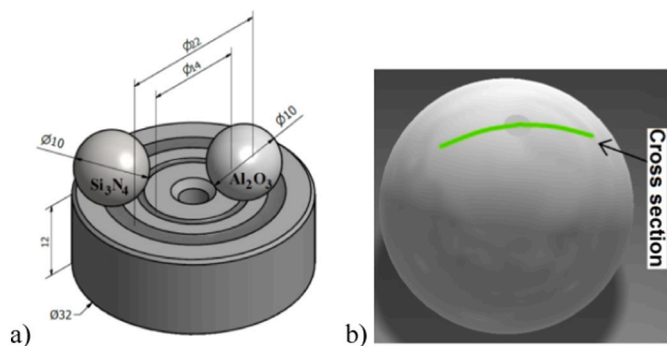


**Fig. 3.** An example of a sample used during the ball-on-disc tests with (a) $A_2O_3$ and $Si_3N_4$ counterbodies and (b) scheme measurement of 2-D transverse profiles on counterbody in the wear trace areas.

**Table 3**
Parameters of ball-on-disc tests carried out against $Al_2O_3$ and $Si_3N_4$ counterbodies.

| Parameter | Value |
|---|---|
| $Al_2O_3$ ball diameter | 10.0 mm |
| Radius of the sliding circles for $Al_2O_3$ ball | 7.0 mm |
| $Si_3N_4$ ball diameter | 10.0 mm |
| Radius of the sliding circles for $Si_3N_4$ ball | 11.0 mm |
| Applied load | 25.0 N |
| Sliding speed | 0.1 m/s |
| Sliding distance | 2000 m |
| Test duration | $2 \cdot 10^4$ s |
| Temperature during tests | 25 °C ± 2 °C |
| Lubrication system | without a lubricant |

2-D transverse profiles in the wear trace areas on the counterbody samples were also carried out (see Fig. 3b).

## 3. Results

### 3.1. Characterization of substrate tool steels

The SEM images of cross-sectional micrographs and XRD pattern for the tool steels examined after heat treatment are shown in Fig. 4. In both cases, carbide particles are observed within a fine tempered martensite matrix. Differences are seen in the size and uniformity distribution of carbides, identified using XRD analysis. Significant differences in microhardness of both types of carbides were observed: 2500–3000 $HV_{0.02}$ for V rich MC type, and 1200–1900 $HV_{0.02}$ for Cr rich $M_7C_3$ [28].

Fig. 5 shows the Raman spectrum of Sverker 21 steel after T + B160 + VN + DLC surface treatment. A peak at about 1550 $cm^{-1}$ was observed, which confirms the presence of diamond and DLC phases in the deposited coating. Peak D is the disordered carbon content and peak G is the graphitic carbon content. This suggests a mixed $sp^2$ and $sp^3$ carbon structure. Heavily broadened lines indicate an amorphous structure of the coating [29–32].

SEM cross-sections of grounded specimens and after two combinations of the sequential turning-burnishing-vacuum nitriding-DLC process are shown in Fig. 6. The thickness of the DLC coating was ≈ 2.5 μm for both steel grades. Uniform coating thickness deposited on steel substrates for both mentioned variants was observed.

### 3.2. Mechanical properties and surface morphology of treated surfaces

Fig. 7 illustrates the microhardness variation along the diffusion zone on both investigated tool steels subjected to the T + B130 + VN + DLC and T + B160 + VN + DLC processes. A significant increase of microhardness compared to the core material was observed for both variants. The depth of the nitriding zone was around 100 μm, with slightly higher values of microhardness in the case of the T + B160 + VN + DLC variant. The results indicated the efficiency of nitriding, resulting in improved load support before the DLC coating application.

Values of hardness (H), Young modulus (E) and H/E ratio for DLC coating deposited on both steels are presented in Fig. 8. No significant change of mechanical properties was observed for both surface treatment variants on conventional Sverker 21 steel (Fig. 8a). Meanwhile, almost a 25% increase of average H and a 12% increase of E was measured for the T + B160 + VN + DLC process (Fig. 8b).

The critical load data from progressive load micro-scratch tests in the range of 0.03 to 5 N are shown in Table 4. The critical loads (Lc) were determined by the acoustic emission method [33–35]. The critical force corresponding to the cohesive fracture $L_{c1}$ and adhesive force $L_{c2}$ can be correlated with the quality of the bond between the coating and the substrate. Damage of the coating initiated from its cohesive failure; for Sverker 21 steel it appeared after reaching loads of 1.34 N and 1.16 N, respectively, for the T + B130 + VN + DLC and T + B160 + VN + DLC
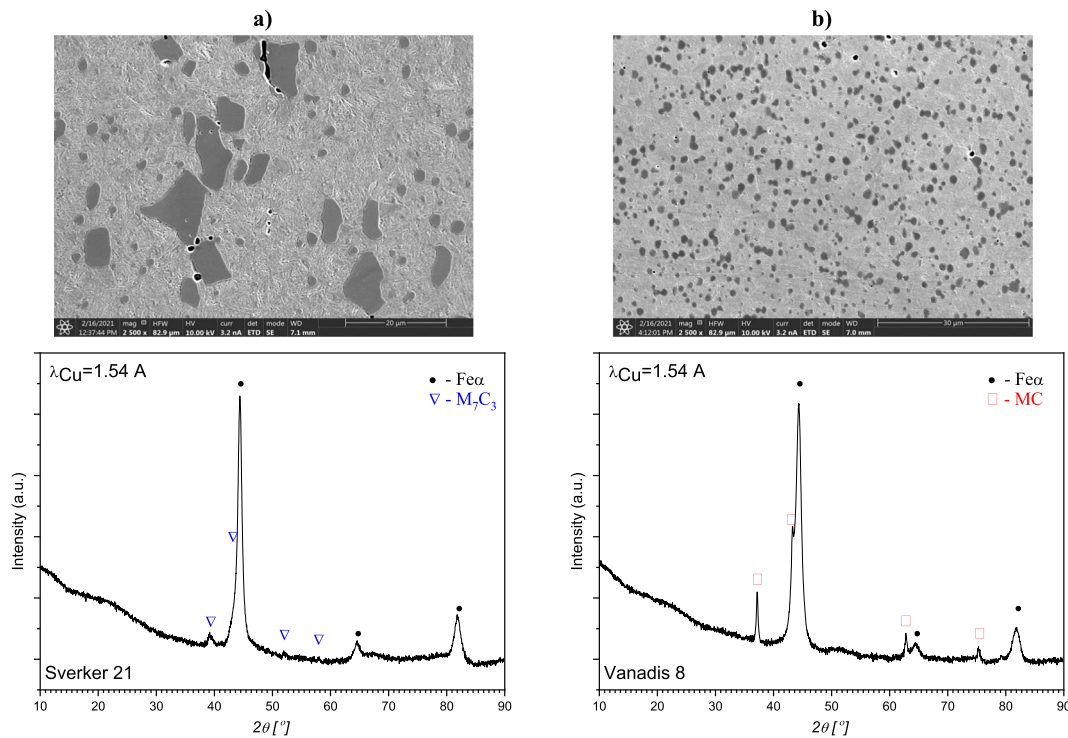
**Fig. 4.** Microstructure of (a) Sverker 21 and (b) Vanadis 8 tool steels with XRD patterns for investigated samples after heat treatment.
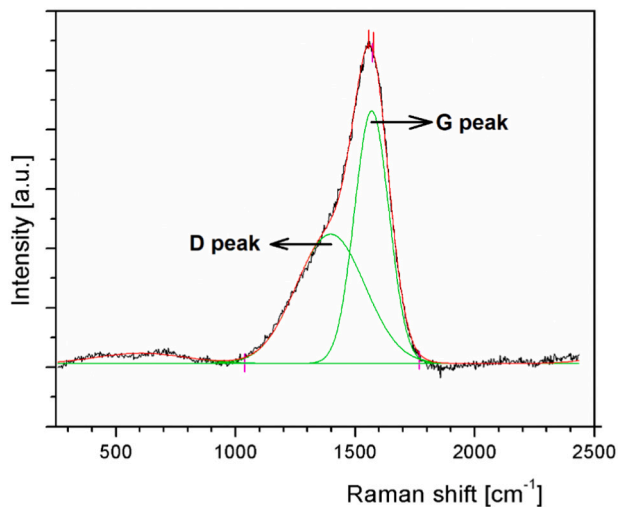


**Fig. 5.** Raman spectrum for the DLC coating deposited on Sverker 21 steel sample (T + B160 + VN + DLC variant).

variants. For Vanadis 8 steel samples, values of $L_{c1}$ were 35% lower for the T + B130 + VN + DLC variant compared to Sverker 21 steel. Meanwhile, analogous comparison for T + B160 + VN + DLC variant shows about 10% higher values for Vanadis 8 steel. The highest values of $L_{c2}$ (total failure in front of the probe) were determined after the T + B160 + VN + DLC variant for both investigated steels. For the variant with a burnishing force of 130 N, values of $L_{c2}$ were 34% and 12% lower, respectively, for Sverker 21 and Vanadis 8 steels.

Tables 5 and 6 present the measured values of selected surface roughness parameters with corresponding 3D topographies and contour line maps of investigated tool steels after the three variants of surface treatment. The lowest surface roughness values were obtained after grinding, for both steels. After carrying out a sequential process with a burnishing force of 130 N and 160 N, the surface roughness slightly

increases, but with regard to forming or cutting tools, it is at an acceptable level.

### 3.3. Tribological experiments

#### 3.3.1. Substrate tool steels

Wear rates and dynamic friction values for Sverker 21 and Vanadis 8 steel samples subjected to grinding are given in Fig. 9. Significant differences in wear resistance between examined steels were determined against the $Al_2O_3$ counterbody – in this case, steel obtained through the P/M technique was characterized by almost an 18-times greater wear resistance. The same trend was found for the $Si_3N_4$ counterbody, but in this case, less than a four-fold difference was achieved. In terms of dynamic friction, Sverker 21 steel samples after grinding showed similar trends for tests against both counterbodies with slightly lower average values observed for $Si_3N_4$. Very similar values of the dynamic friction were recorded in tests against $Al_2O_3$ and $Si_3N_4$ counterbodies for Vanadis 8 steel after grinding. Differences in the course of dynamic friction were recorded only in the initial stage of the test.

Examples of 3D wear tracks for grounded samples of investigated tool steels after ball-on-disc tests against $Al_2O_3$ and $Si_3N_4$ counterbodies are presented in Fig. 10. Wear traces for both steels were wider and deeper after tests using the $Al_2O_3$ counterbody. The main wear mechanism observed in this case was abrasive wear. On the other hand, adhesive wear dominated tests using the $Si_3N_4$ counterbody.

#### 3.3.2. Surface treated Sverker 21

Results of wear rates and dynamic friction values for Sverker 21 tool steel subjected to a sequential four-stage surface treatment in two variants (with a burnishing force of 130 N and 160 N applied prior vacuum nitriding) are presented in Fig. 11. No significant difference in wear resistance in tests against $Al_2O_3$ and $Si_3N_4$ counterbodies were found for the T + B130 + VN + DLC variant. With regard to the dynamic friction, in the case of the $Al_2O_3$ counterbody, only slightly lower values were recorded. However, a significant increase in wear resistance was observed for a sequential process with the burnishing force of 160 N
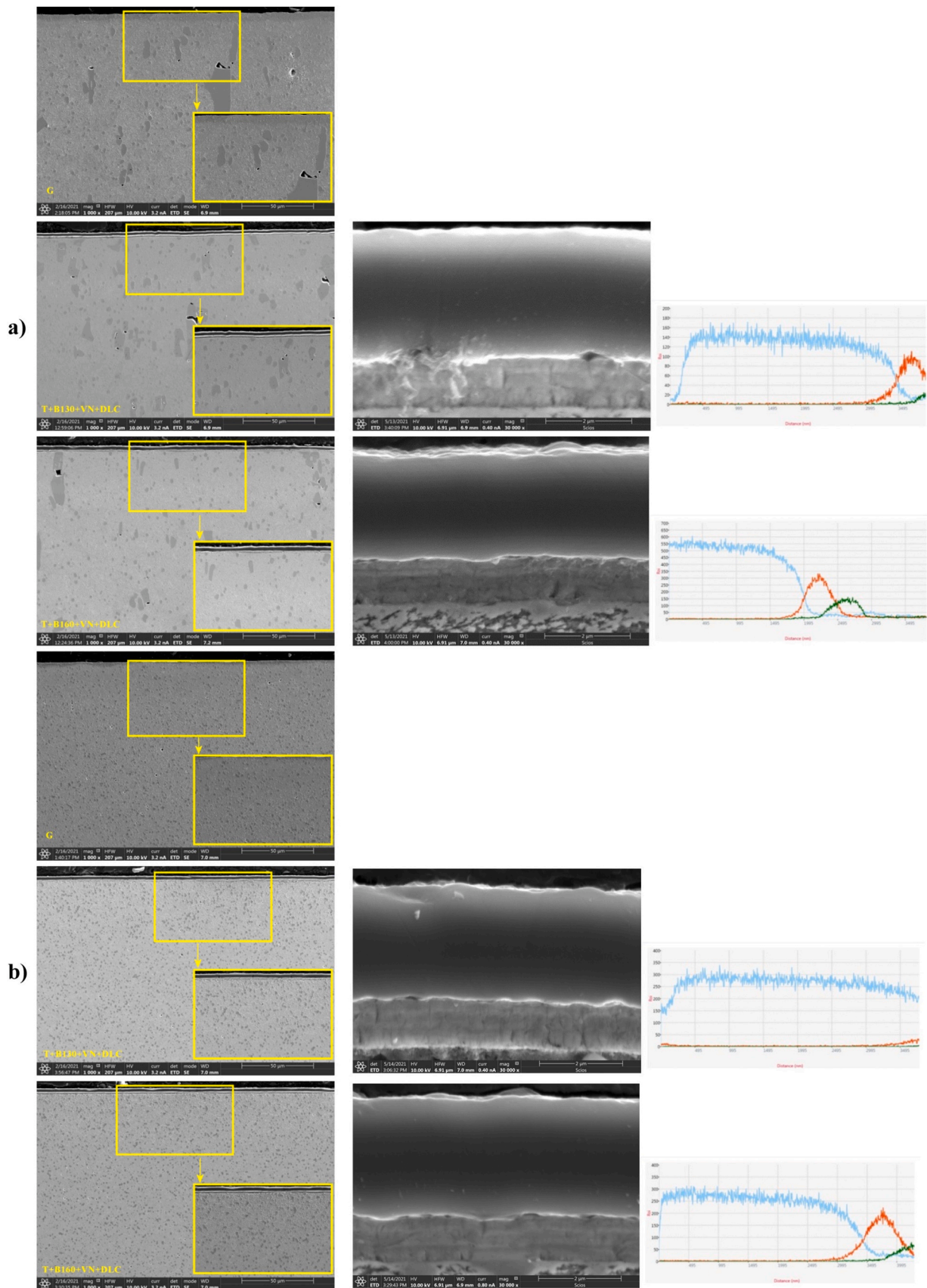
**Fig. 6.** SEM microstructure of surface layer samples of (a) Sverker 21 and (b) Vanadis 8 tool steels after selected surface treatment processes.
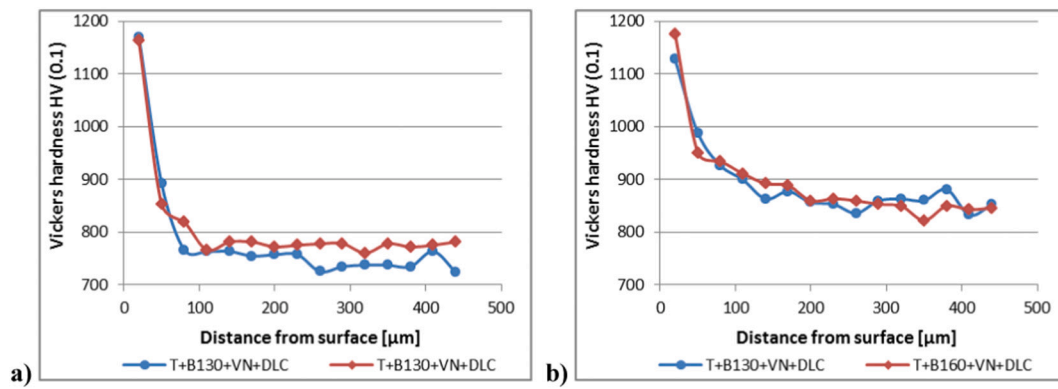
**Fig. 7.** Changes in microhardness along the diffusion zone of Sverker 21 (a) and Vanadis 8 (b) specimens after T + B130 + VN + DLC and T + B160 + VN + DLC.
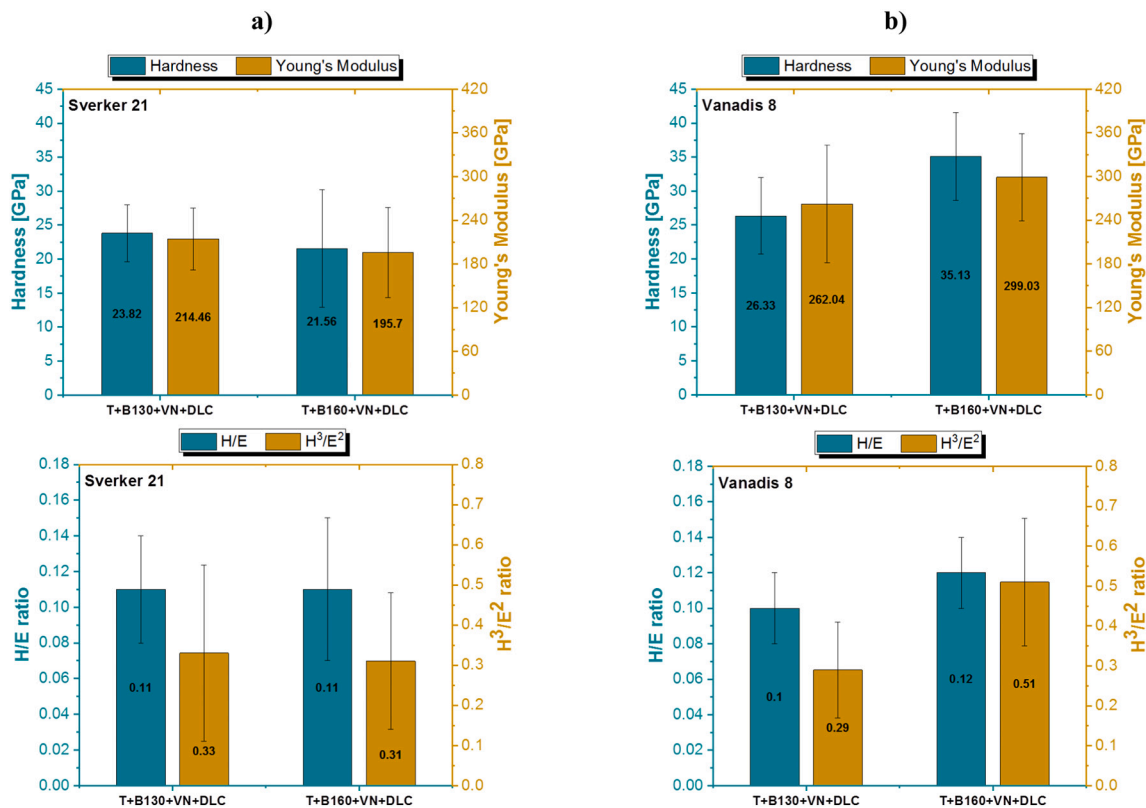


**Fig. 8.** Hardness (H), Young's modulus (E), H/E and H3/E2 ratios for DLC coating deposited in T + B130 + VN + DLC and T + B160 + VN + DLC variants on (a) Sverker 21 and (b) Vanadis 8 steel.

**Table 4**
Results of scratch tests for samples of investigated tools steels.

| Steel | Surface treatment | Scratch tests | | | | |
|---|---|---|---|---|---|---|
| | | Load [N] | $L_{c1}$ [N] | $H_{C1}$ [µm] | $L_{c2}$ [N] | $H_{max}$ [µm] |
| Sverker 21 | G | – | – | – | – | – |
| | T + B130 + VN + DLC | 0.03 to 5 | 1.34 | 1 | 1.63 | 2 |
| | T + B160 + VN + DLC | 0.03 to 5 | 1.16 | 1 | 2.46 | 2.5 |
| Vanadis 8 | G | – | – | – | – | – |
| | T + B130 + VN + DLC | 0.03 to 5 | 0.87 | 1 | 1.81 | 2 |
| | T + B160 + VN + DLC | 0.03 to 5 | 1.30 | 3 | 2.05 | 2 |

prior to nitriding. The average value of the wear rate in case of the $Al_2O_3$ counterbody reached 0.13, an increase of over 97% of wear resistance comparing to the 130 N burnishing force. The much lower value of dynamic friction should also be emphasized in this case. Comparison of the results for the $Si_3N_4$ counterbody shows a 24% improvement in wear resistance after carrying out the T + B160 + VN + DLC variant.
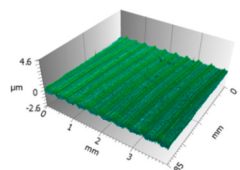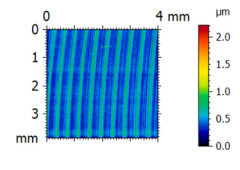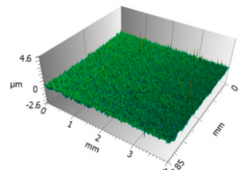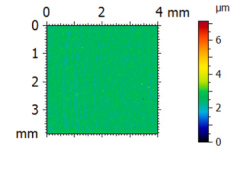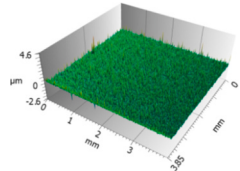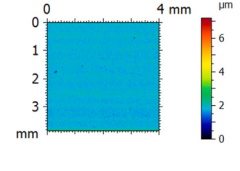
3D topographies of the wear tracks along with SEM images for Sverker 21 steel after selected processes of surface treatments are shown in Fig. 12. The observed wear mechanism for the considered variants after tests against the $Al_2O_3$ counterbody was abrasive wear.

*3.3.3. Surface treated Vanadis 8*

Summarized results of wear rates and dynamic friction for Vanadis 8 tool steel samples after T + B130 + VN + DLC and T + B160 + VN + DLC variants are shown in Fig. 13. The average value of wear rate for combination with the burnishing force of 160 N in case of P/M steel is very
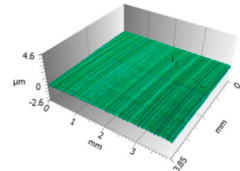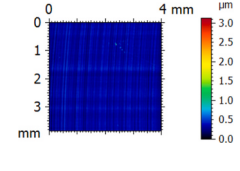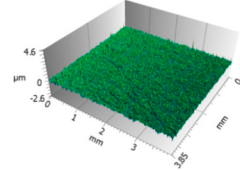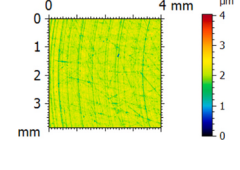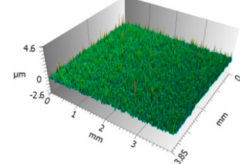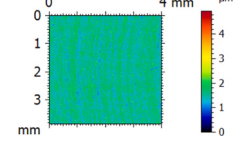
**Table 5**

Mean values of surface roughness parameters with 3D topographies and contour line maps of Sverker 21 tool steel after selected surface treatment processes.

| Surface treatment | Surface roughness parameters (μm) | | | | 3D topographies and contour line maps |
| --- | --- | --- | --- | --- | --- |
| | Sa | Sz | Sp | Sv | |
| G | 0.13 | 2.08 | 1.58 | 0.50 |  |
| T + B130 + VN + DLC | 0.17 | 7.14 | 4.58 | 2.56 |  |
| T + B160 + VN + DLC | 0.11 | 4.73 | 2.89 | 1.84 |  |

**Table 6**

Mean values of surface roughness parameters with 3D topographies and contour line maps of Vanadis 8 tool steel after selected surface treatment processes.

| Surface treatment | Surface roughness parameters (μm) | | | | 3D topographies and contour line maps |
| --- | --- | --- | --- | --- | --- |
| | Sa | Sz | Sp | Sv | |
| G | 0.05 | 3.12 | 2.75 | 0.37 |  |
| T + B130 + VN + DLC | 0.12 | 4.04 | 1.92 | 2.12 |  |
| T + B160 + VN + DLC | 0.16 | 4.94 | 3.39 | 1.56 |  |

similar to the one obtained for Sverker 21 after the same sequential treatment (see Fig. 11). It should be noted that overall, Vanadis 8 steel is characterized by better wear resistance than Sverker 21; values of about 30% lower wear rates were observed for the T + B130 + VN + DLC variant.

3D topographies of the wear tracks along with SEM images for Vanadis 8 steel after two applied sequential processes of surface layer modification are shown in Fig. 14. A characteristic irregular wear track was observed in tests against the $Si_3N_4$ counterbody for the T + B160 + VN + DLC variant. On the other hand, a uniform and shallow wear track was observed against the $Al_2O_3$ counterbody after the same surface treatment. This corresponds with a low value of the dynamic friction, as shown in Fig. 13.

## 4. Discussion

The dynamic friction and wear behaviour of two pre-treated variant tool steels (Sverker 21 and Vanadis 8) coated by DLC were investigated. Lauwers et al. [36] demonstrated that combined processes involving at least two methods of surface treatment have positive effects on the micromechanical properties of the surface layer. Such processes can include surface modification through slide diamond burnishing with gas nitriding, which significantly affects the structure and phase composition of the surface layer of martensitic tool steels, as shown in the author's own research [37,38].

It should be noted that the durability of the components is determined not only by the properties of the substrate (such as hardness), but also the hardness gradient throughout the applied coating system.
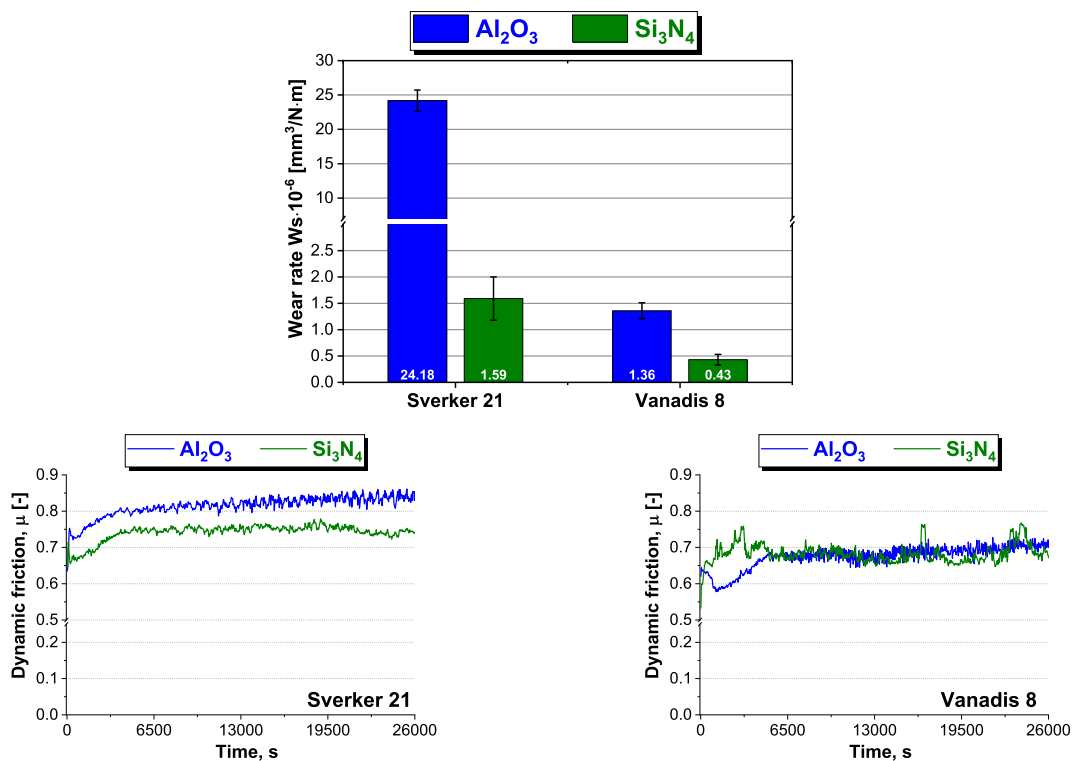
**Fig. 9.** Values of wear rates and dynamic friction for samples of examined tool steels after grinding; ball-on-disc tests against Al$_2$O$_3$ and Si$_3$N$_4$ counterbodies.
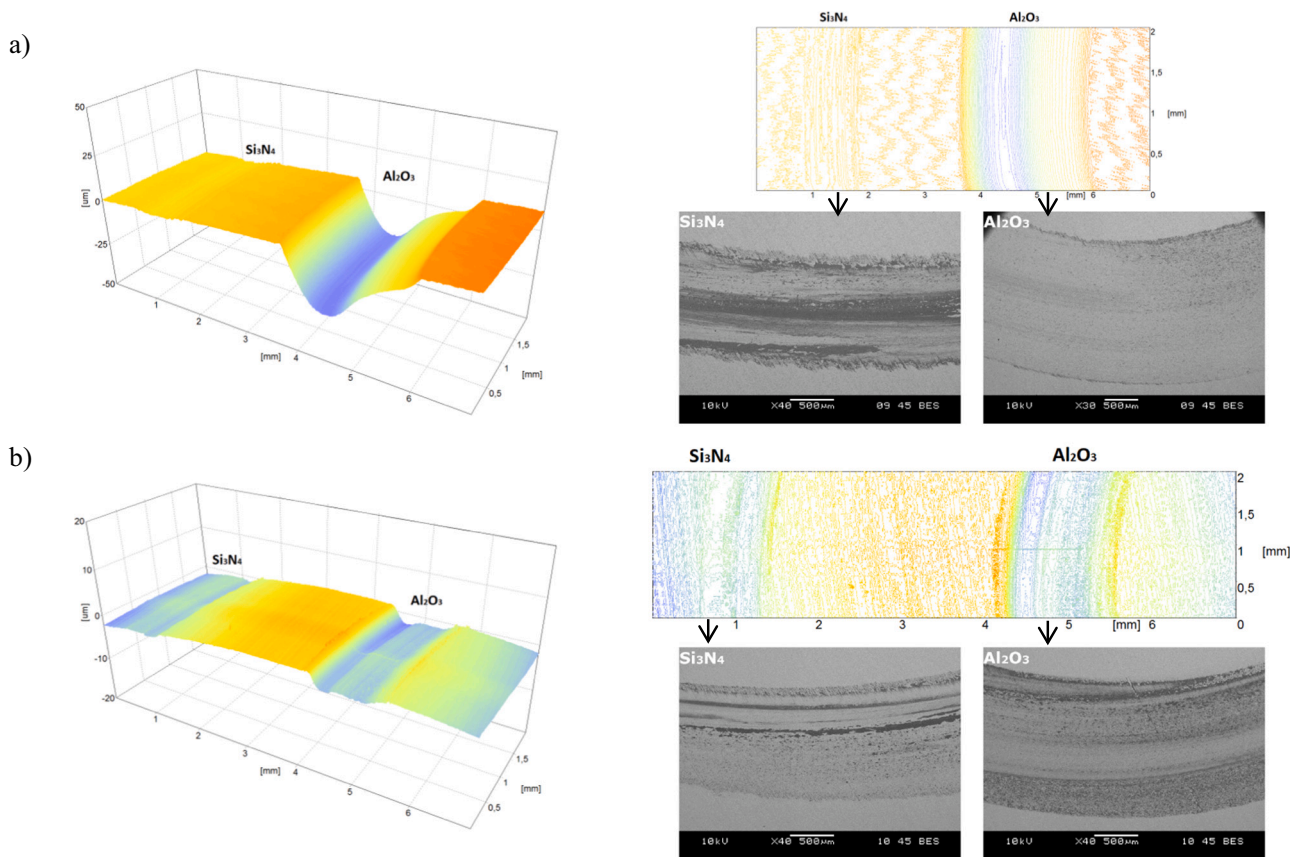


**Fig. 10.** Wear tracks for samples of examined tool steels after grinding (a) Sverker 21 and (b) Vanadis 8; ball-on-disc tests against Al$_2$O$_3$ and Si$_3$N$_4$ counterbodies.

**Fig. 11.** Values of wear rates and dynamic friction for samples of Sverker 21 tool steel after T + B130 + VN + DLC and T + B160 + VN + DLC; ball-on-disc tests against (a) $Al_2O_3$ and (b) $Si_3N_4$ counterbodies.



**Fig. 12.** Wear tracks for samples of Sverker 21 tool steel after (a) T + B130 + VN + DLC and (b) T + B160 + VN + DLC; ball-on-disc tests against $Al_2O_3$ and $Si_3N_4$ counterbodies.

**Fig. 13.** Values of wear rates and dynamic friction for samples of Vanadis 8 tool steel after T + B130 + VN + DLC and T + B160 + VN + DLC; ball-on-disc tests against (a) Al$_2$O$_3$ and (b) Si$_3$N$_4$ counterbodies.
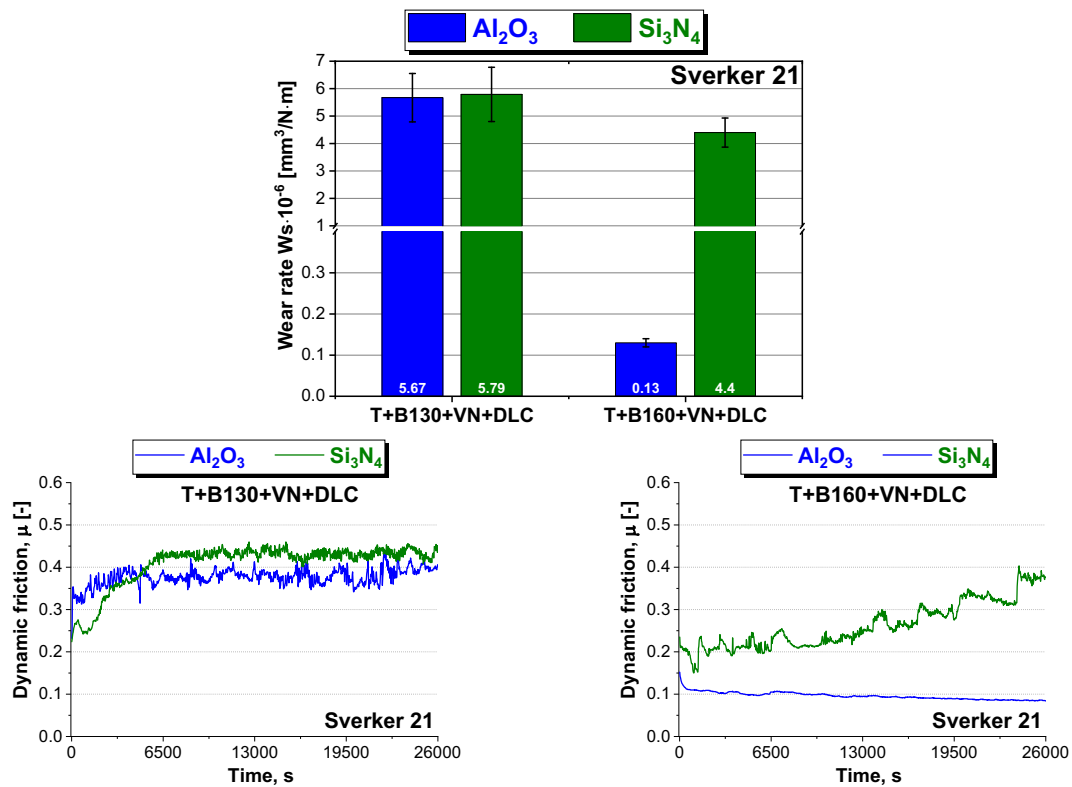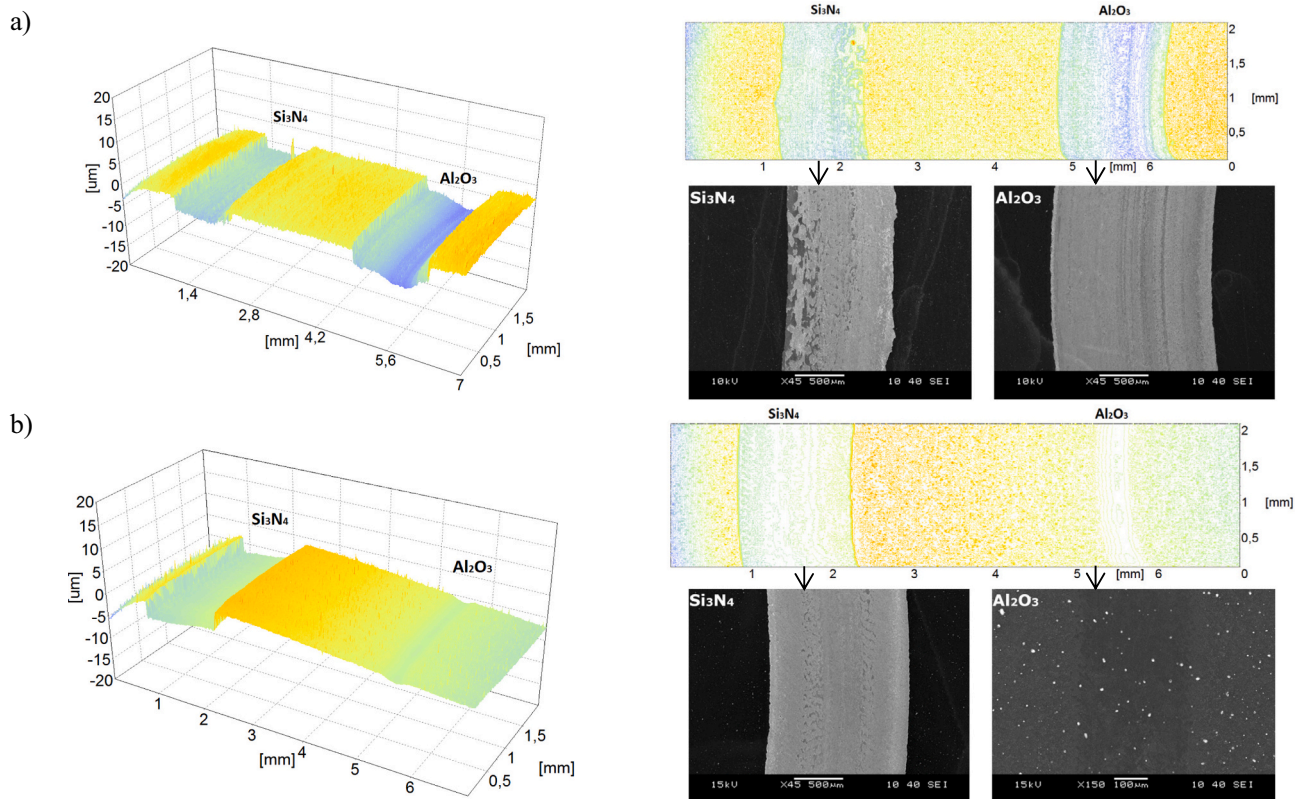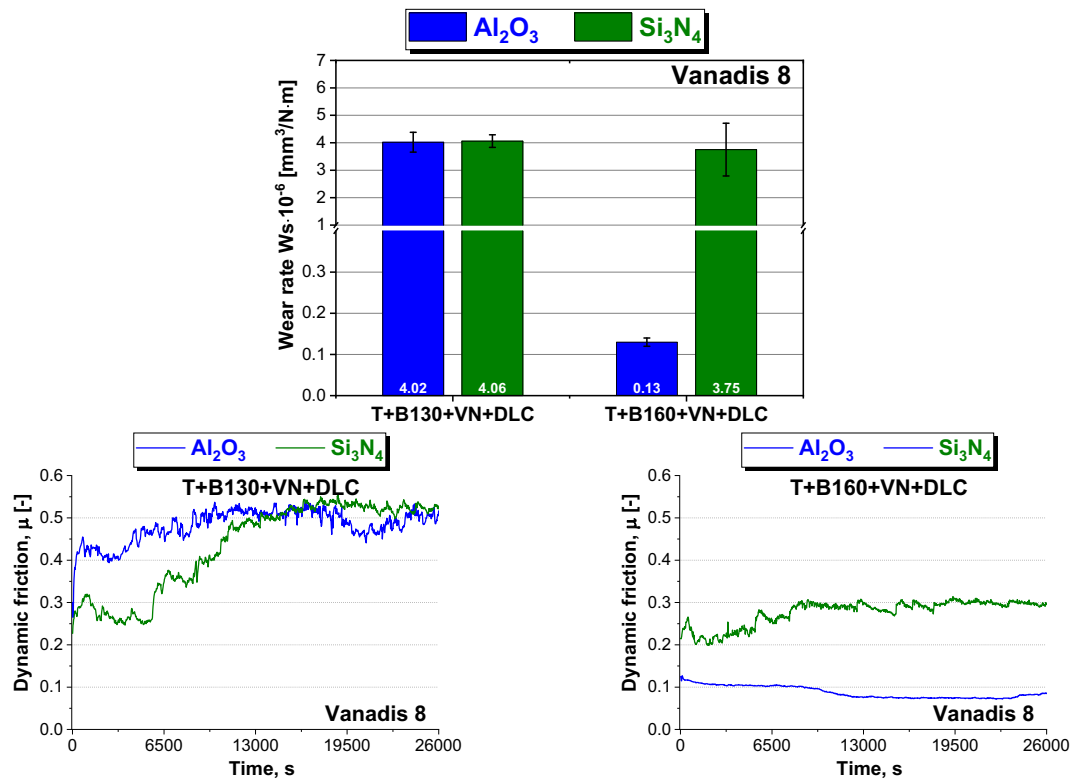


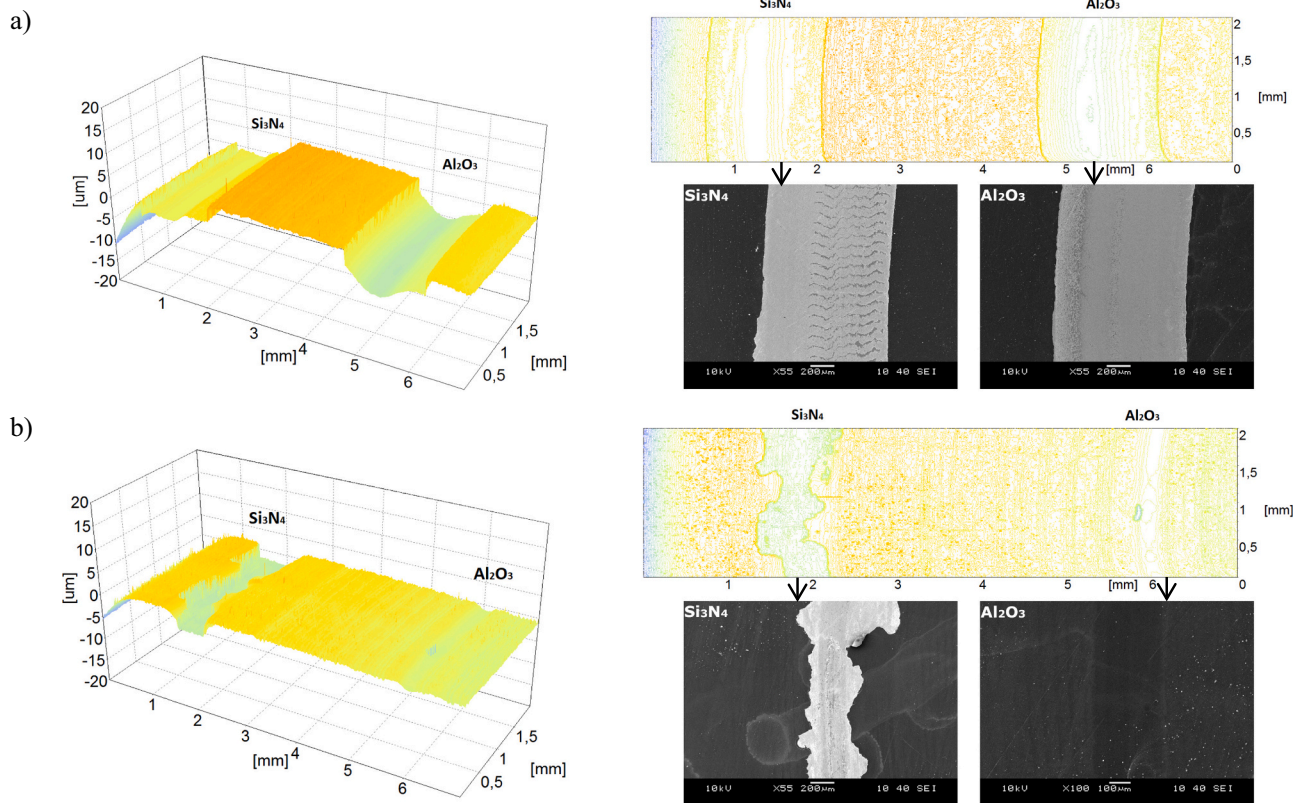**Fig. 14.** Wear tracks for samples of Vanadis 8 tool steel after (a) T + B130 + VN + DLC and (b) T + B160 + VN + DLC; ball-on-disc tests against Al$_2$O$_3$ and Si$_3$N$_4$ counterbodies.

Therefore, the durability of components subjected to extreme loads depends on the appropriate selection of the substrate and the functional coating's properties.

For both steels, carrying out the T + B160 + VN + DLC treatment variant contributed to obtaining the lowest values of wear rates after tests against an $Al_2O_3$ counterbody. Furthermore, the DLC coating deposited on steel substrate previously burnished with 160 N force and subsequently vacuum nitrided exhibited as friction values as low as 0.10 (see Figs. 11 and 13). In contrast, reduction of the burnishing force to 130 N in an analogous sequential process (T + B130 + VN + DLC) led to much higher values of dynamic friction ~0.40 and ~ 0.50, for Sverker 21 and Vanadis 8 tool steels, respectively. The higher friction is attributed to the poor adhesion of the DLC coatings determined for the T + B130 + VN + DLC variant, as found in scratch tests (Table 4). Tillmann et al. [39] came to similar conclusions, considering the duplex treatment, consisting of plasma nitriding and DLC coating on the hot-work tool steel AISI H11. Moreover, the authors highlighted the delamination of the DLC layer, which led to insufficient tribological protection, resulting in high coefficients of friction as well as high wear rates [39]. In relation to the results of wear resistance in our study, the trends are especially visible for tests carried out after the application of the T + B130 + VN + DLC process. The wear mechanism with coating delamination was evidenced by SEM analysis. An example of the wear track with EDS analysis for Sverker 21 steel sample subjected to T + B130 + VN + DLC, after ball-on-disc tests against an $Si_3N_4$ counterbody is shown

in Fig. 15. Two distinctive areas in the wear track (marked red and green) were identified and subsequently subjected to EDS analysis. Spectra 5 and 6 (image in green frame) indicate a pure DLC coating, while for spectrum 4, a high content of C, Si and Cr was identified in the Sverker 21 steel substrate. The lack of N should also be noted. This is an evidence for a fragment of Cr layer exposed under the DLC coating. Moreover, the area/position in the wear track where these scans were taken confirms that the Cr coating was present. Spectra 1 and 2 (image in red frame) show a high content of Si with a lower amount of C (but still higher than in the steel substrate). For these spectra, no N was again determined. Hence, due to the lack of Cr in this area, it cannot be considered as a fragment of the Cr thin layer. The mesh of micro-cracks visible in this area is noteworthy. This seems to be attributed to the repeated/cyclic rotation of the sample in relation to the $Si_3N_4$ ball, the contact area of which changed with increasing wear, thereby changing the contact pressure. Meanwhile, this type of damage/failure does not occur at the edges of the wear track, which can be explained by the geometry of the $Si_3N_4$ counterbody. The quality of machining should also be considered. Surface roughness parameters, such as Sa and Sz, were respectively 25% and 18% higher for Sverker 21 steel samples subjected to T + B130 + VN + DLC compared to the T + B130 + VN + DLC variant. The higher roughness combined with the long test time (more than 7 h) may have contributed to uneven wear of DLC coating and, thus, the observed delamination.

According to Podgornik et al. [40], from the point of view of tool life



| Spectrum | C | N | O | Al | Si | Cr | Fe | Total |
|---|---|---|---|---|---|---|---|---|
| 1 | 4.7 | | 47.4 | 0.8 | 19.7 | | 27.3 | 100.0 |
| 2 | 5.9 | | 46.3 | 0.8 | 19.8 | | 27.2 | 100.0 |
| 3 | | 1.3 | | | 0.4 | 12.9 | 85.5 | 100.0 |
| 4 | | 1.2 | | | 0.3 | 13.8 | 84.7 | 100.0 |

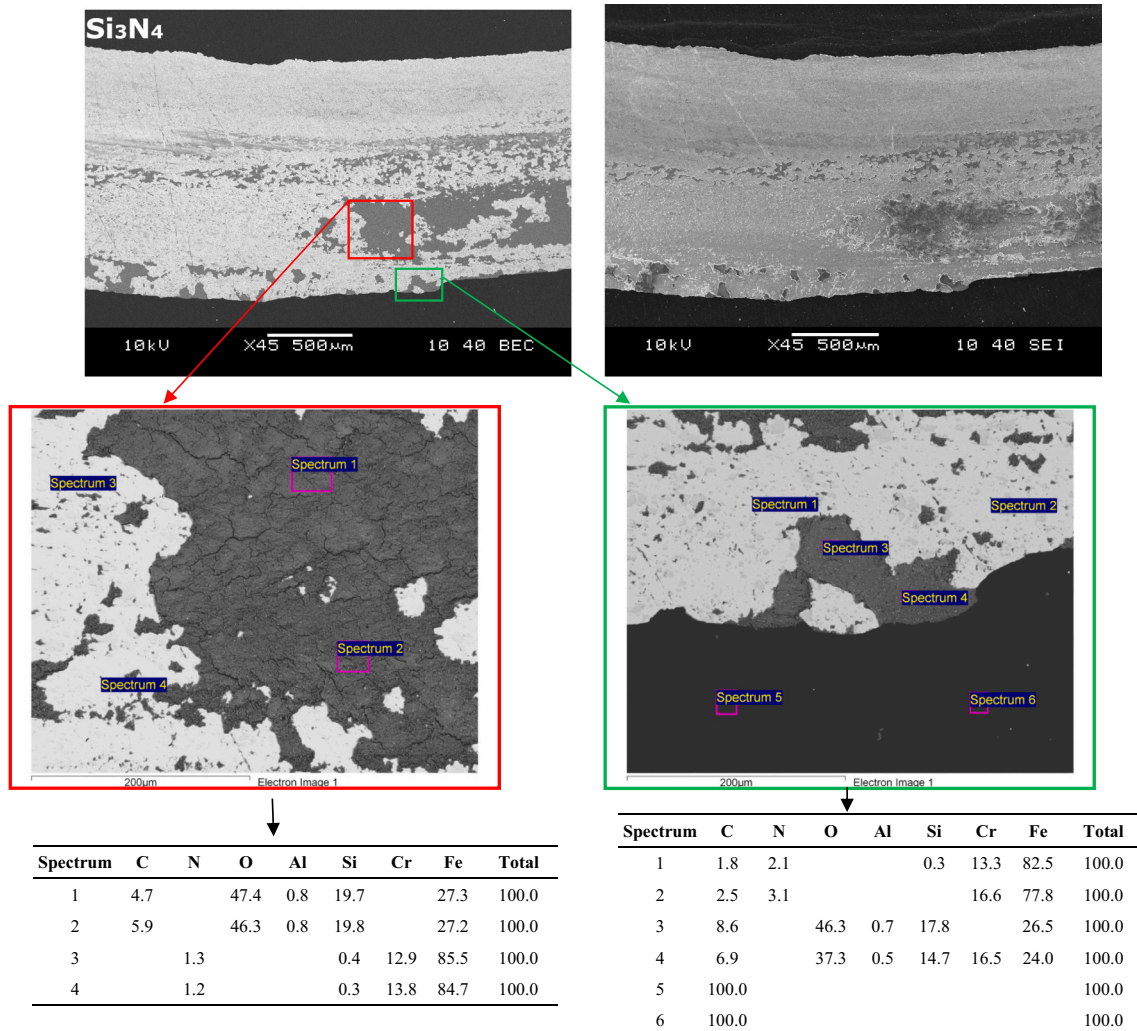| Spectrum | C | N | O | Al | Si | Cr | Fe | Total |
|---|---|---|---|---|---|---|---|---|
| 1 | 1.8 | 2.1 | | | 0.3 | 13.3 | 82.5 | 100.0 |
| 2 | 2.5 | 3.1 | | | | 16.6 | 77.8 | 100.0 |
| 3 | 8.6 | | 46.3 | 0.7 | 17.8 | | 26.5 | 100.0 |
| 4 | 6.9 | | 37.3 | 0.5 | 14.7 | 16.5 | 24.0 | 100.0 |
| 5 | 100.0 | | | | | | | 100.0 |
| 6 | 100.0 | | | | | | | 100.0 |

**Fig. 15.** SEM wear track with EDS analysis for sample of Sverker 21 tool steel after T + B130 + VN + DLC; ball-on-disc tests against $Si_3N_4$ counterbodies.

as well as workpiece surface quality, the DLC coating with its excellent anti-sticking properties and sufficiently good wear resistance represents the best solution for forming tool applications of austenitic stainless steel.

The relationship between the H/E and $H^3/E^2$ ratios and the wear resistance of DLC coating were also analysed (Fig. 8). The first ratio relates to elasticity, while the second is typically used as an indicator of resistance to plastic deformation in a loaded contact [41,42]. It should be added that it is possible to adjust the wear resistance of a solid by adapting its elastoplastic properties, by increasing the hardness or decreasing the elastic modulus, as reported by Claver et al. [41].

For both steels, the highest values of H/E and $H^3/E^2$ ratios were achieved for DLC coatings deposited in the T + B160 + VN + DLC process. These values correlate with the results of tribological tests against $Al_2O_3$ and $Si_3N_4$ counterbodies (see Figs. 11 and 13).

The SEM cross-sectional images of the investigated samples after chemical etching are shown in Fig. 16. Nitrided compound layer formation has been extensively described elsewhere [43–47]. Novák et al. [48] described it as follows: the process starts with ionization of the nitrogen–hydrogen atmosphere in the glow discharge forming N+ or NH+ ions. These charged particles bombard the surface of steel, which results in sputtering of iron, carbon and alloying elements. Consequently, metastable FeN nitrides are formed by reactions in gaseous state, followed by their deposition on the surface. The solid-state reaction of the deposited nitrides with the substrate produces $Fe_4N$ nitrides and/or $Fe_{2-3}(C,N)$ carbonitrides. In addition, the ions which are discharged in contact with the surface are adsorbed on the material surface and consequently diffuse inward the material. As a result, the second sub-layer, the diffusion zone, grows. The diffusion zone comprises a solid solution of nitrogen in martensite and fine nitride precipitate.

The compound layer and a diffusion zone formed during nitriding are visible in Fig. 16. For both applied sequential variants, the diffusion zone consists of a nitrogen solid solution in martensite and of fine nitrides. The nitrided case depth was determined from the microhardness profiles

(see Fig. 7) and reached around 100 μm, with slightly higher values of microhardness for the T + B160 + VN + DLC variant, as mentioned earlier. Nitriding has an impact on the tool steel bulk toughness and may affect fatigue life of the tool [49]. However, in our case, the overall tool performance/life should be assessed by considering the durability of the coating as well. Hence, if the coating can be adequately supported by the plasma nitrided surface, the improvement of the tribological properties of the coating-substrate system (i.e., tool) can be expected.

Finally, considering correlations between the wear of counterbodies and the dynamic friction, some observations can be made. Examples of 2-D transverse profiles of $Al_2O_3$ and $Si_3N_4$ counterbodies in the wear trace areas with corresponding wear volume values are presented in Fig. 17. Lower dynamic friction obtained in the T + B160 + VN + DLC variant, ∼ 0.1 and ∼0.3, respectively, for $Al_2O_3$ and $Si_3N_4$ counterbodies (see Fig. 13), correlate with lower wear of the counterbodies compared to the T + B130 + VN + DLC treatments. Moreover, a 14-fold lower wear of the $Al_2O_3$ counterbody was observed after tests against samples subjected to a sequential process with 160 N compared to 130 N.

## 5. Conclusions

Based on the experimental results the following conclusions can be formulated:

1. The choice of surface preparation method significantly affects the durability of the applied coating-substrate system, defined by friction and wear, as well as the H/E and $H^3/E^2$ ratios of deposited DLC coating. Thus, there is a potential possibility of qualitatively and quantitatively forming the surface layer in order to obtain its expected properties in industrial conditions.
2. The best wear resistance against the $Al_2O_3$ counterbody was achieved for samples subjected to the following treatment: turning + burnishing with 160 N force + vacuum nitriding + DLC coating; the
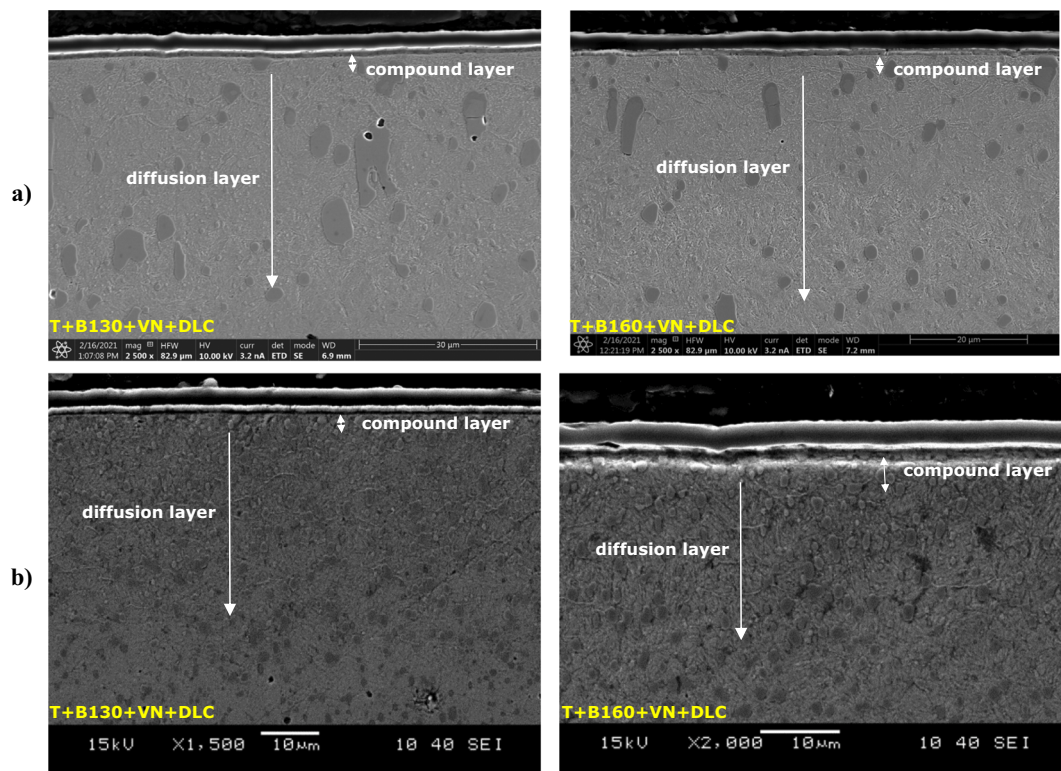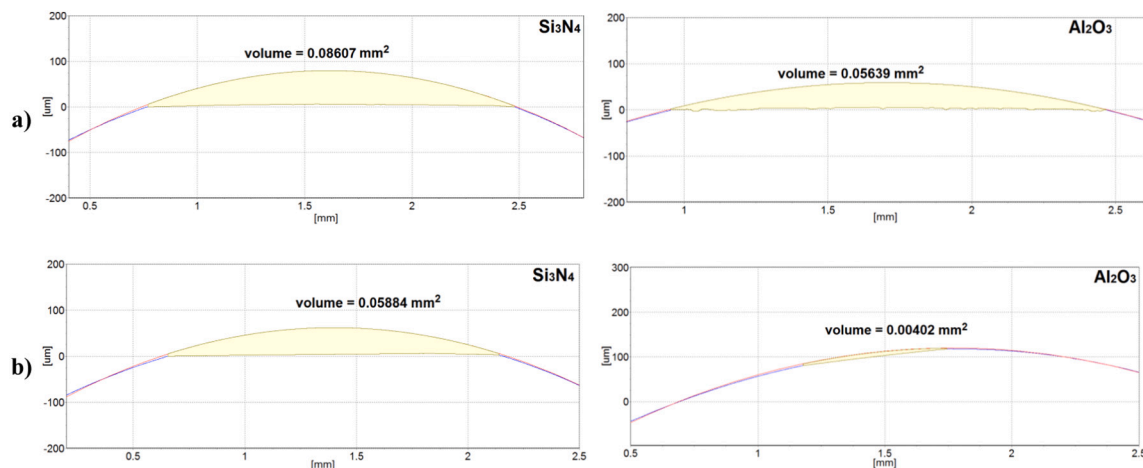


**Fig. 16.** SEM microstructures of surface layer samples after T + B130 + VN + DLC and T + B160 + VN + DLC treatments for (a) Sverker 21 and (b) Vanadis 8 tool steels.

**Fig. 17.** Examples of 2-D transverse profiles of $Al_2O_3$ and $Si_3N_4$ counterbodies in the wear trace areas; after the tests with samples of Vanadis 8 tool steel subjected: (a) T + B130 + VN + DLC and (b) T + B160 + VN + DLC.

wear resistance is more than 99% and 90% greater than after grinding, respectively, for Sverker 21 and Vanadis 8 tool steels.

3. The lowest values of dynamic friction of around 0.1 were recorded after the T + B160 + VN + DLC treatment variant for both steel substrates.

4. A similar trend of dynamic friction for Sverker 21 steel samples after grinding can be observed for both counterbodies. Slightly lower average values were observed for the $Si_3N_4$ counterbody. Very similar values and trends of dynamic friction were recorded for Vanadis 8 steel samples after grinding, with minor differences in the initial test stages.

5. The highest values of H/E and $H^3/E^2$ ratios determined for DLC coating deposited in the T + B160 + VN + DLC variant have been achieved for powder metallurgy steel.

**Declaration of competing interest**

The authors declare that they have no known competing financial interests or personal relationships that could have appeared to influence the work reported in this paper.

**Acknowledgments**

**References**

[1] Global Global Metal Cutting Tools Market By Material (Carbide; Ceramics; CBN & PCD; Others), By Process (Milling; Turning; Drilling; Rotary; Others), By End-Use (Automotive; Aerospace & Defense; Energy; Others), By region, competition, Forecast & Oppor., 2024. Report for the ReportBuyer. https://www.prnewswire.com/news-releases/global-metal-cutting-tools-market-was-valued-at-22-2-billion-in-2018-and-is-projected-to-grow-at-a-cagr-of-8-8-to-reach-38-3-billion-by-2024–300867570.html, 2019 (accessed 15 February 2021).
[2] H. Caliskan, P. Panjan, C. Kurbanoglu, 3.16 hard coatings on cutting tools and surface finish, in: M.S.J. Hashmi (Ed.), Comprehensive Materials Finishing, Elsevier, Oxford, 2017, pp. 230–242, https://doi.org/10.1016/B978-0-12-803581-8.09178-5.
[3] A. Inspektor, P.A. Salvador, Architecture of PVD coatings for metalcutting applications: a review, Surf. Coat. Technol. 257 (2014) 138–153, https://doi.org/10.1016/j.surfcoat.2014.08.068.
[4] K. Bobzin, High-performance coatings for cutting tools, CIRP J. Manuf. Sci. Technol. 18 (2017) 1–9, https://doi.org/10.1016/j.cirpj.2016.11.004.
[5] L. Lind, P. Peetsalu, P. Podra, E. Adoberg, R. Veinthal, P. Kulu, Description of punch wear mechanism Turing fine banking process. Proceedings of 7th International DAAAM Baltic Conference "Industrial Engineering", 22–24 April 2010, Tallin.
[6] F. Klocke, E. Brinksmeier, K. Weinert, Capability profile of hard cutting and grinding processes, CIRP Ann. Manuf. Technol. 54 (2005) 22–45, https://doi.org/10.1016/S0007-8506(07)60018-3.
[7] G.L. Nicola, F.P. Missell, R.P. Zeilmann, Surface quality in milling of hardened H13 steel, Int. J. Adv. Manuf. Technol. 49 (2010) 53–62, https://doi.org/10.1007/s00170-009-2382-3.
[8] F. Klocke, O. Dambon, B. Behrens, Analysis of defect mechanisms in polishing of tool steels. Prod. Eng. 5 (2011)475–483. doi:https://doi.org/10.1007/s11740-011-0301-6.
[9] M. Okada, M. Shinya, H. Matsubara, H. Kozuka, H. Tachiya, N. Asakawa, M. Otsu, Development and characterization of diamond tip burnishing with a rotary tool, J. Mater. Process. Technol. 244 (2017) 106–115, https://doi.org/10.1016/j.jmatprotec.2017.01.020.
[10] A. Saldaña-Robles, H. Plascencia-Mora, E. Aguilera-Gómez, A. Saldaña-Robles, A. Marquez-Herrera, A.J. Diosdado-Dela la Peña, Influence of ball-burnishing on roughness, hardness and corrosion resistance of AISI 1045 steel, Surf. Coat. Technol. 339 (2018) 191–198, https://doi.org/10.1016/j.surfcoat.2018.02.013.
[11] A. Heydari Astaraee, S. Bagherifard, A. Bradanini, P. Duó, S. Henze, B. Taylor, M. Guagliano, Application of shot peening to case-hardened steel gears: the effect of gradient material properties and component geometry, Surf. Coat. Technol. 398 (2020), 126084, https://doi.org/10.1016/j.surfcoat.2020.126084.
[12] K. Żak, W. Grzesik, M. Prażmowski, Investigation of sequential cryogenic hard turning and ball burnishing processes, Metalurgija 53 (2014) 521–525. https://hrcak.srce.hr/122178.
[13] W. Tillmann, M. Dildrop, T. Sprute, Influence of nitriding parameters on the tribological properties and the adhesion of Ti- and Cr-based multilayer designs, Surf. Coat. Technol. 260 (2014) 380–385, https://doi.org/10.1016/j.surfcoat.2014.09.017.
[14] F. Czerwinski, Thermochemical treatment of metals, in: F. Czerwinski (Ed.), Heat Treatment – Conventional and Novel Applications, in Tech, 2012, pp. 73–102, https://doi.org/10.5772/5156r6.
[15] S.-H. Chang, Y.-C. Wen, K.-T. Huang, C.-M. Liu, Optimization of DLC films on oxynitriding-treated Vanadis 10 tool steel through the various duty cycles of DC-pulsed plasma-enhanced CVD. Kovove Mater. 59 (2021) 109–118. DOI: https://doi.org/10.4149/km2021 2 109.
[16] Y. Duan, S. Qu, X. Li, Effect of quench-tempering conditions prior to nitriding on microstructure and fretting wear mechanism of gas nitrided X210CrW12 steel, Surf. Coat. Technol. 25 (2019) 247–258, https://doi.org/10.1016/j.surfcoat.2018.12.066.
[17] J.C. Avelar-Batista, E. Spain, G.G. Fuentes, A. Sola, R. Rodriguez, J. Housden, Triode plasma nitriding and PVD coating: a successful pre-treatment combination to improve the wear resistance of DLC coatings on Ti6Al4V alloy, Surf. Coat. Technol. 201 (2006) 4335–4340, https://doi.org/10.1016/j.surfcoat.2006.08.070.
[18] M. Folea, A. Roman, N.-B. Lupulescu, An overview of DLC coatings on cutting tools performance, Acad. J. Manuf. Eng. 8 (2010) 30–36.
[19] D.N. Awang Shri, J. Ramli, N.A. Alang, M.M. Mahat, Influence of surface pretreatment on carbon coating of cutting tools using PVD, Appl. Mech. Mater. 236-237 (2012) 530–535, https://doi.org/10.4028/www.scientific.net/AMM.236-237.530.

[20] J. Miyamoto, P. Abraha, The effect of plasma nitriding treatment time on the tribological properties of the AISI H13 tool steel, Surf. Coat. Technol. 375 (2019) 15–21, https://doi.org/10.1016/j.surfcoat.2019.07.001.

[21] D. Toboła, W. Brostow, K. Czechowski, P. Rusek, I. Wronska, Structure and properties of burnished and nitrided AISI D2 tool steel, Medziagotyra 21 (2015) 511–516, https://doi.org/10.5755/j01.ms.21.4.7224.

[22] J.T. Maximov, G.V. Duncheva, A.P. Anchev, M.D. Ichkova, Slide burnishing—review and prospects, Int. J. Adv. Manuf. Technol. 104 (2019) 785–801, https://doi.org/10.1007/s00170-019-03881-1.

[23] J.T. Maximov, G.V. Duncheva, A.P. Anchev, V.P. Dunchev, J. Capek, A cost-effective optimization approach for improving the fatigue strength of diamond-burnished steel components, J. Braz. Soc. Mech. Sci. Eng. 43 (2021) 33, https://doi.org/10.1007/s40430-020-02723-6.

[24] S.J. McMaster, T.W. Liskiewicz, A. Neville, B.D. Beake, Probing fatigue resistance in multi-layer DLC coatings by micro- and nano-impact: correlation to erosion tests, Surf. Coat. Technol. 402 (2020), 126319, https://doi.org/10.1016/j.surfcoat.2020.126319.

[25] G.M. Pharr, W.C. Oliver, Measurement of thin film mechanical properties using nanoindentation, MRS Bull. 17 (1992) 28–33, https://doi.org/10.1557/S0883769400041634.

[26] W. Brostow, H.E. Hagg Lobland, Materials: Introduction and Applications, John Wiley & Sons, New York, NY, USA, 2017.

[27] Ł. Janczewski, D. Toboła, W. Brostow, K. Czechowski, H.E. Hagg Lobland, M. Kot, K. Zagórski, Effects of ball burnishing on surface properties of low density polyethylene, Tribol. Int. 93 (2016) 36–42, https://doi.org/10.1016/j.triboint.2015.09.006.

[28] P. Nurthen, O. Bergman, I. Hauer, Carbide design in wear resistant powder materials. PM 2008 World Congress in Washington, USA, June 10 (2008), pp. 1–16.

[29] N. Paik, Raman and XPS studies of DLC films prepared by a magnetron sputter-type negative ion source, Surf. Coat. Technol. 200 (2005) 2170–2174, https://doi.org/10.1016/j.surfcoat.2004.08.073.

[30] W.G. Cui, Q.B. Lai, L. Zhang, F.M. Wang, Quantitative measurements of sp3 content in DLC films with Raman spectroscopy, Surf. Coat. Technol. 205 (2010) 1995–1999, https://doi.org/10.1016/j.surfcoat.2010.08.093.

[31] X. Shi, T.W. Liskiewicz, B.D. Beake, J. Chen, Ch.Wang, Tribological performance of graphite-like carbon films with varied thickness. Tribol. Int. 149 (2020) 105586. doi:https://doi.org/10.1016/j.triboint.2019.01.045.

[32] H. Kovacı, Ö. Baran, A.F. Yetim, Y.B. Bozkurt, L. Kara, A. Çelik, The friction and wear performance of DLC coatings deposited on plasma nitrided AISI 4140 steel by magnetron sputtering under air and vacuum conditions, Surf. Coat. Technol. 349 (2018) 969–979, https://doi.org/10.1016/j.surfcoat.2018.05.084.

[33] M. Łepicka, M. Grądzka-Dahlke, D. Pieniak, K. Pasierbiewicz, A. Niewczas, Effect of mechanical properties of substrate and coating on wear performance of TiN- or DLC-coated 316LVM stainless steel, Wear 382-383 (2017) 62–70, https://doi.org/10.1016/j.wear.2017.04.017.

[34] A. Ghiotti, S. Bruschi, Tribological behaviour of DLC coatings for sheet metal forming tools, Wear 271 (2011) 2454–2458, https://doi.org/10.1016/j.wear.2010.12.043.

[35] B.D. Beake, T.W. Liskiewicz, V.M. Vishnyakov, M.I. Davies, Development of DLC coating architectures for demanding functional surface applications through nano- and micro-mechanical testing, Surf. Coat. Technol. 284 (2015) 334–343, https://doi.org/10.1016/j.surfcoat.2015.05.050.

[36] B. Lauwers, F. Klocke, A. Klink, A.E. Tekkaya, R. Neugebauer, D. Mcintosh, Hybrid processes in manufacturing, CIRP Ann. Manuf. Technol. 63 (2014) 561–583, https://doi.org/10.1016/j.cirp.2014.05.003.

[37] D. Toboła, W. Brostow, K. Czechowski, P. Rusek, Improvement of wear resistance of some cold working tool steels, Wear 382-383 (2017) 29–39, https://doi.org/10.1016/j.wear.2017.03.023.

[38] D. Toboła, B. Kania, Phase composition and stress state in the surface layers of burnished and gas nitrided AISI D2 and Vanadis 6 tool steels, Surf. Coat. Technol. 353 (2018) 105–115, https://doi.org/10.1016/j.surfcoat.2018.08.055.

[39] W. Tillmann, N.F. Lopes Dias, D. Stangier, Influence of plasma nitriding pretreatments on the tribo-mechanical properties of DLC coatings sputtered on AISI H11, Surf. Coat. Technol. 357 (2019) 1027–1036, https://doi.org/10.1016/j.surfcoat.2018.11.002.

[40] B. Podgornik, S. Hogmark, O. Sandberg, V. Leskovsek, Wear resistance and anti-sticking properties of duplex treated forming tool steel, Wear 254 (2003) 1113–1121, https://doi.org/10.1016/S0043-1648(03)00322-3.

[41] A. Claver, E. Jiménez-Piqué, J.F. Palacio, E. Almandoz, J. Fernández de Ara, I. Fernández, J.A. Santiago, E. Barba, J.A. García, Comparative study of tribomechanical properties of HiPIMS with positive pulses DLC coatings on different tools steels, Coatings 11 (2021) 28, https://doi.org/10.3390/coatings11010028.

[42] A. Leyland, A. Matthews, On the significance of the H/E ratio in wear control: a nanocomposite coating approach to optimised tribological behaviour, Wear 246 (2000) 1–11, https://doi.org/10.1016/S0043-1648(00)00488-9.

[43] T. Lampe, S. Eisenberg, G. Laudien, Compound layer formation during plasma nitriding and plasma nitrocarburising, Surf. Eng. 9 (1) (1993) 69–76, https://doi.org/10.1179/sur.1993.9.1.69.

[44] A. Leyland, K.S. Fancey, A. Matthews, Plasma nitriding in a low pressure triode discharge to provide improvements in adhesion and load support for wear resistant coatings, Surf. Eng. 7 (3) (1991) 207–215, https://doi.org/10.1179/sur.1991.7.3.207.

[45] C. Zhao, C.X. Li, H. Dong, T. Bell, Study on the active screen plasma nitriding and its nitriding mechanism, Surf. Coat. Technol. 201 (2006) 2320–2325, https://doi.org/10.1016/j.surfcoat.2006.03.045.

[46] H. Aghajani, M. Torshizi, M. Soltanieh, A new model for growth mechanism of nitride layers in plasma nitriding of AISI H11 hot work tool steel, Vacuum 141 (2017) 97–102, https://doi.org/10.1016/j.vacuum.2017.03.032.

[47] A. Moreno-Bárcenas, J.M. Alvarado-Orozco, J.M. González Carmona, G.C. Mondragón-Rodríguez, J. González-Hernández, A. García-García, Synergistic effect of plasma nitriding and bias voltage on the adhesion of diamond-like carbon coatings on M2 steel by PECVD, Surf. Coat. Technol. 374 (2019) 327–337, https://doi.org/10.1016/j.surfcoat.2019.06.014.

[48] P. Novák, D. Vojtěch, J. Šerák, Wear and corrosion resistance of a plasma-nitrided PM tool steel alloyed with niobium, Surf. Coat. Technol. 200 (2006) 5229–5236, https://doi.org/10.1016/j.surfcoat.2005.06.023.

[49] A. Celik, S. Karadeniz, Improvement of the fatigue strength of AISI 4140 steel by an ion nitriding process, Surf. Coat. Technol. 72 (1995) 169–173, https://doi.org/10.1016/0257-8972(94)02348-4.